Int. J. Electrochem. Sci., 17 **(2022)** Article Number: 220216, doi: 10.20964/2022.02.24

International Journal of
ELECTROCHEMICAL
SCIENCE
www.electrochemsci.org

Short Communication

Corrosion inhibition properties of the oil extracted from the leaves of *Eruca sativa* for carbon steel in acidic medium

H. A. Alrafai

Department of Chemistry, College of Science, King Khalid University, P. O. Box 9004, Postal Code 61413, Abha, Kingdom of Saudi Arabia
*E-mail: halrafai@kku.edu.sa

Received: 14 October 2021 / *Accepted:* 26 November 2021 / *Published:* 5 January 2022

The aim of the current research is to explore the potential corrosion inhibitory properties of the natural oil extracted from *Eruca sativa* leaves (OESL) on carbon steel (CS) in HCl (1.0 M). Scanning electron microscopy (SEM) was used for studying the surface morphological changes of carbon steel (CS) samples. Various experimental techniques such as mass loss and electrochemical techniques were employed to investigate the efficiency of OSEL as corrosion inhibitor. The adsorption nature of the OSEL onto the carbon steel surface was found to follow the Langmuir isotherm model. Furthermore, the data obtained from the electrochemical experiments indicated that the OSEL inhibitor behaves as a mixed-type inhibitor.

Keywords: Eruca sativa; Oil; Inhibitor; Carbon steel; HCl

1. INTRODUCTION

Alloys and metals are commonly used in numerous domestic and industrial applications such as oil, bio-chemical, desalination and paints industries. These materials however are at risk to severe deterioration due to corrosion. The rigorousness of the corrosion destruction depends on the type of the metal and the corrosion medium. It is well known that acids are known aggressive corrosion media and cause fast and dangerous corrosion of metals and alloys [1]. Acids are usually used in the industrial sector for pickling, de-scaling, and cleaning. Several methods are used to minimize or prevent the corrosion of alloys and metals. One of the most common methods that used to avoid corrosion is the addition of inhibitors because of its high efficiency [2]. Several organic and inorganic compounds have been effectively exploited as corrosion inhibitors. Nevertheless, as an eco-friendly and low-cost materials, natural oil plants as corrosion inhibitors are explored recently. Several plant extracts were used such as, leaves extract of *Centrosema pubescens* [3], extracts of leaf and barks of *Acacia tortilis*

[4], leaf extract of *Juniperus procera* [5], Various Parts of *Rotula Aquatica* Plant [6] leaves of (Mahogany) *Khaya senegalensis* [7] garlic extract [8], *azadirachta indica* extract [9] and *Coleus forskohlii* leaf extract [10].

Oils extracted from different plants have reported several times to have efficient anti-corrosion properties. Oils extracted from *Moringa peregrine* [11], *citrus sinensis* [12], black piper [13] and castor seeds [14] have been used as efficient corrosion inhibitors for carbon steel in various corrosive media.

The majority of these investigations were conducted in the presence of several acids for instance, HNO_3, HCl, and H_2SO_4. The anti-corrosion properties of these extracts can be ascribed to the presence of constituents that have hetero atoms such as O, N and S. These atoms are reported to be adsorption centres because of the presence of π or conjugated bonds structures.

The aim of this work is to examine the efficacy of the natural oil which extracted from the leaves of *Eruca sativa* (OESL) as corrosion inhibitor. To the best of my knowledge, no research on the role of the oil extracted from the leaves of *Eruca sativa* has been reported. The different interactions between OESL and the CS surface in an aggressive corrosive medium (HCl 1M) are investigated in the current study using various techniques such as Potentiodynamic Polarization, Electrochemical impedance Spectroscopy and Scanning Electron Microscopy.

2. EXPERIMENTAL

2.1. Extraction of OESL

The oil was extracted from *Eruca sativa leaves* (250 g) using methanol (80%) as a solvent. The extraction procedure followed the previously described method [15]. Methanol was evaporated under reduced pressure and the oil was kept in the fridge at 4^{o}C till used.

The desired concentrations of the inhibitor were prepared by dissolving the required weight in 1.0 M HCl.

2.2. Carbon steel samples and corrosive solutions

The composition (wt%) of the carbon steel (CS) samples used in this work is as follows: C (0.45), Mn (0.71), Si (0.32), S (0.04), P (0.03), Cr (0.43), Cu (0.31), Al (0.12), and balance Fe. The CS samples were abraded using various grades of emery papers. The abraded CS samples were then rinsed using double-distilled water and acetone. The required concentrations of HCl were prepared by dilution using double -distilled water.

2.3. Weight loss measurements

The experimental procedures adopted in this work followed the ASTM standards [16]. The CS samples were immersed in both uninhibited and inhibited solutions for 12 hours at 298 K. After each

experiment, the CS samples were taken out of the corrosive media and washed using double -distilled water and acetone, dried and reweighted [17]. All experiments were implemented three times to ensure the reliability and reproducibility of the results.

2.4. Electrochemical measurements

All tests were performed using AuotoLab (model N101). A three-electrode cell composed of a saturated reference electrode (Ag/AgCl), a working electrode (CS) having surface area of 0.32 cm^2 that was immersed in HCl (1.0 M) and a platinum (Pt) auxiliary or counter electrode. To reach an equilibrium, the CS samples were dipped in the corrosive test solution for 45 mins before the electrochemical measurements. The electrochemical impedance (EIS) tests were performed within 0.1 mHz to 10 mHz frequency range and an AC amplitude of 5 mV. The Potentiodynamic polarization (PDP) measurements were performed within -850 to -100 mV potential range using scanning rate of 1 mV s^{-1} .

2.5. SEM studies

Scanning electron microscopy (SEM) was adopted to investigate the CS surface morphology in the presence and absence of 2.5 g/L of the inhibitor. The SEM tests were performed adopting a Hitachi TM-1000 system with an accelerating voltage of 15 kV. The immersion time for all tests was always 6 hours.

3. RESULTS AND DISCUSSION

3.1. Weight loss measurements

The inhibition efficacy (IE_{ML}%) of OESL is calculated using Equation X [18]:

$$IE_{ML}\% = \frac{ML^o - ML}{ML^o} \times 100 \quad (1)$$

where ML^o and ML signify the corrosion rates without and with OESL, respectively.

Table 1. Corrosion behaviour of carbon steel with and without different concentrations of OESL by using mass loss method at 298K

OESL	OESL (g/L)	Mass loss (g)	EI_{ML} (%)	Θ
Blank	---	1.653	----	
OESL	0.50	0.587	64.5	0.645
	1.00	0.452	72.7	0.727
	1.50	0.310	81.2	0.812
	2.00	0.205	87.5	0.875
	2.50	0.082	95.0	0.950

It is obvious from the results displayed in Table1 that at low OESL concentration, minor effect on corrosion rate was observed and as OESL concentration increased, the corrosion rate is considerably decreased. The inhibition properties of OESL is most likely due to its strong affinity towards iron atoms. At high OESL concentrations more coverage of CS surface is achieved [19-21]. The inhibitor exhibited the maximum $IE_{ML}\%$ (95.0%) at 2.5 g/L.

3.2. Electrochemical tests

Electrochemical methods are widely used to find important data about the interactions that may occur at the inhibitor/metal interface. Electrochemical tests are usually performed for alloys and/or metal samples exposed to corrosive medium in the with and without OESL.

Potentiodynamic polarization technique (PDP) was used to evaluate the inhibition properties of OESL and the results are shown in Figure 1. The kinetic data obtained from PDP are displayed in Table 2. The inhibition efficacy ($IE_{PDP}\%$) is determined by Equation (2) [11]:

$$IE_{PDP}\% = \left[1 - \frac{i_{corr}}{i^{o}_{corr}}\right] \times 100 \qquad (2)$$

where, i_{corr} and i^{o}_{corr} are the corrosion current densities in the presence and absence of OESL.

Table 2. Data obtained from the PDP plots without and with different concentrations of OESL at 298K

	Conc. g/L	- E_{corr} (mV vs. SCE)	i_{corr} (μA cm^{-2})	β_a (mV dec^{-1})	β_c (mV dec^{-1})	IE%
Blank	---	491	443	84	156	
OESL	0.50	502	157	92	133	64.7
	1.00	494	126	81	147	71.4
	2.00	497	55	97	139	87.8
	2.50	493	24	85	172	94.6

Results show that the current densities of both cathode and anode decreased after the adding of OESL.

Phytochemical screening of the *Eruca sativa* leaves revealed the presence of glycosides, fixed oils, alkaloids, terpenoids, tannin, phenolic compounds and flavonoids [19]. Due to the adsorption of these constituents, this variation became more noticeable as the concentration of OESL increases, probably because of the blocking of several of the active sites on the CS surface. Furthermore, Table 2 reveals that the addition of the different concentrations of OESL has slight effect on the values of the corrosion potential (E_{corr}) demonstrating that OESL is a mixed type inhibitor [20] and hence it can be concluded that, the reaction mechanism remained constant although the available surface area for H_2 evolution was significantly decreased and the access of H^+ to the CS surface became more hard [21-23]. Results from the PDP tests are in good agreement with that obtained by the mass loss method.

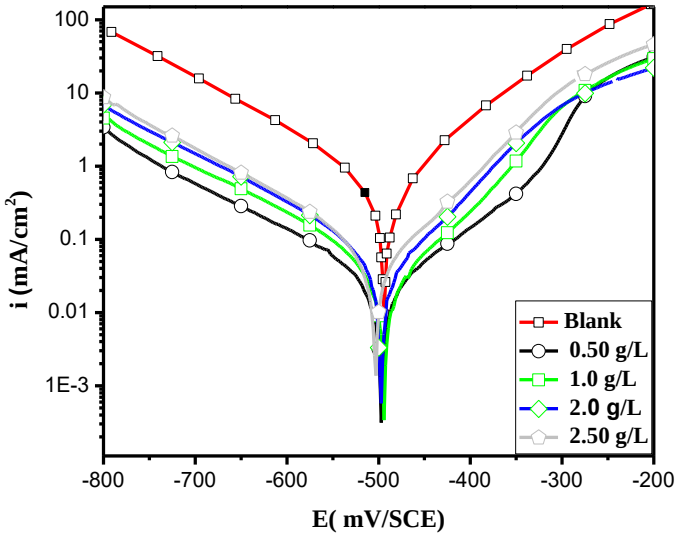

Figure 1. PDP plots of CS in 1.0 M HCl without and with various concentrations of OESL at 298K

The open circuit potential (OCP) plots were recorded for inhibited and uninhibited solutions for 60 mins (until constant potential is obtained).

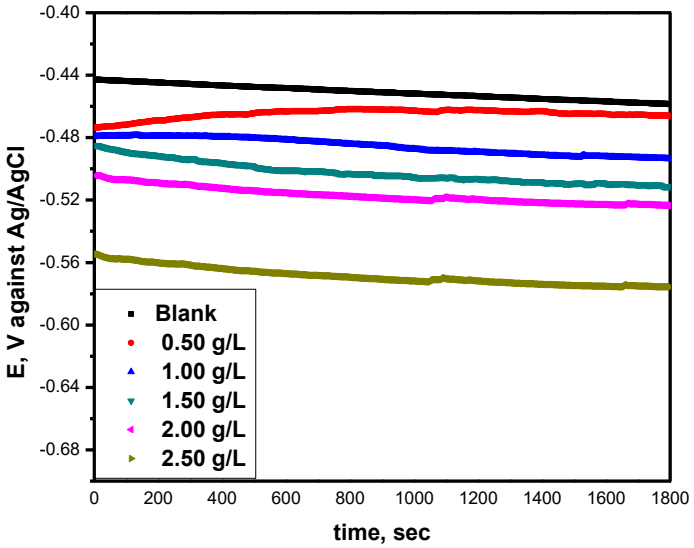

Figure 2. Variation of E_{OCP} with time for CS with and without the various concentrations of OESL at 298K

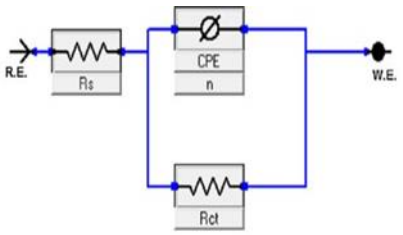

Figure 3. Equivalent circuit model for the analysis of EIS data

Table 3. Results obtained from EIS diagram using different concentration of OESL at 298K

	conc. (g/L)	R_S, (Ω cm^2)	$10^{-3} \times Y_o$ $_\mu \Omega^{-1}$ sn cm^{-1}	N	R_{ct} (Ω cm^2)	% IE_{EIS}
Blank	--	17.4	156.6	0.799	17.7 ± 0.5	-
OESL	0.50	12.7	116.0	0.801	52.1 ± 2.0	66.0
	1.00	11.9	123.3	0.827	68.3 ± 2.9	74.1
	1.50	6.6	77.6	0.866	97.5.5 ± 3.7	81.9
	2.00	7.8	70.8	0.835	151.3 ± 6.4	88.3
	2.50	3.5	70.0	0.827	417.6 ± 15.7	95.8

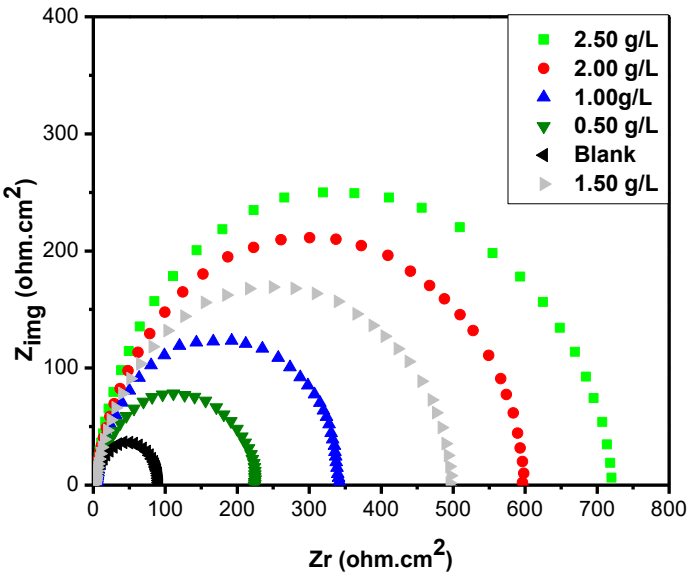

Figure 4. Nyquist spectra using different concentrations of OESL at 298K

These plot are shown in Figure 2. The adopted Electrical Equivalent Circuit (EEC) is shown in Figure 3 while the data collected from electrochemical impedance spectroscopy (EIS) are displayed as Nyquist plots in Figure 4. All the EIS parameters together with the inhibition efficiency $R_{p_{inh}}$ are presented in Table 3. The inhibition efficiency was calculated using equation (3):

$$\%EI_{EIS} = \frac{R_{ct} - R_{ct(inh)}}{R_{ct}} \times 100 \quad (3)$$

where, R_{ct} and $R_{ct(inh)}$ stand for charge-transfer resistances of the CS before and after the OESL addition, respectively.

Analysis of the results revealed that, the plots showed only one depressed capacitive semicircles and this suggests that only one phenomenon happened, and the process of charge transfer is the only active pathway to govern the dissolution of iron at metal/solution interface [11].

The results also show that the impedance response of the CS in the corrosive solution was significantly affected by the addition of OSEL. Figure 4 shows that semicircles increase as the concentration of OSEL increases. The data obtained from EIS tests are presented in Table 3. It is obvious that more OSEL molecules are adsorbed on the CS surface as the concentration of OSEL increases, leading to creation of protecting layer on CS surface [24]. Concurrently, a clear drop was observed in the double layer capacitance in the existence of OESL. This led to alterations in the interface indicative of the better adsorption of the inhibitor on CS surface, and as a result there had been a obvious increase in the thickness of the dielectric double layer that caused minimum dissolution of CS.

3.3. Adsorption isotherm

It is extensively reported that the corrosion inhibition is achieved by adsorbing the inhibitor constituents onto the surface of the metal or alloy [25]. Adsorption can be categorized into three main classes (i) physical (ii) chemical (iii) physicochemical in nature. The adsorption nature can be deduced by examining the experimental data to different isotherm models [11]. The experimental data in the current work were tested using Langmuir, Temkin and Freundlich isotherm models. It was found that the Langmuir model best fitted the experimental data. The linear equation of this model is given by Equation 4[26]:

$$\frac{C_{inh}}{\theta} = \frac{1}{K_{ads}} + C_{inh} \quad (4)$$

where C_{inh} denotes the inhibitor concentration and K_{ads} is the equilibrium constant. The free energy change (ΔG^{o}_{ads}) values were calculated using equation 5:

$$\Delta G^{o}_{ads} = -RTln(K_{ads} \times 55.5) \quad (5)$$

where, R is the universal gas constant (8.314 J/K), T is absolute temperature and the value of 55.5 is the concentration of H_2O in solution in mol L^{-1}.

The plot of C_{inh}/θ *against* C_{inh} gives straight line as shown in Figure 5 with R^2 and slope values close to 1 indicating that the adsorption process follows the Langmuir isotherm model. Values of ΔG^{o}_{ads} and K_{ads} were determined as -14.6 kJ mol^{-1} and 2.52 respectively proving the spontaneous nature of the adsorption process.

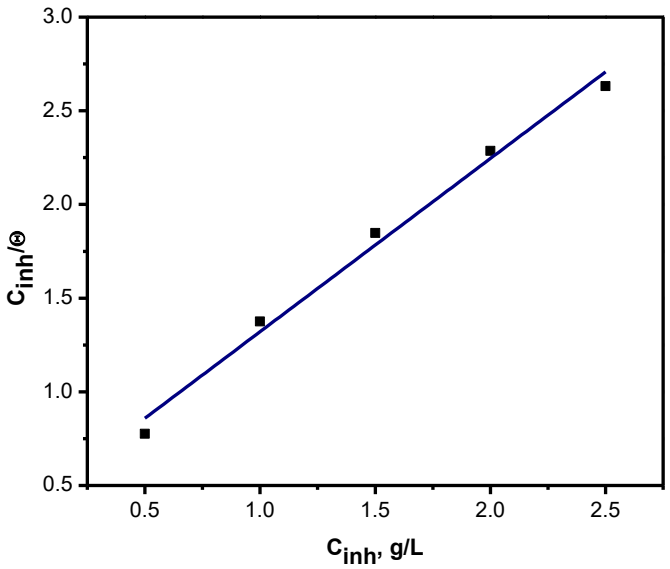

Figure 5. Plot of Langmuir model for CS using different concentrations of OESL at 298K

The results shown that the adsorption process is physical in nature because the ΔG^{o}_{ads} value is lower than -20 kJ mol^{-1}, [13].

3.4 Temperature effect

A series of mass loss experiments were performed at the range of 293–323 K with and without of 2.5g of OESL. The effect of temperature on the inhibition efficiency was investigated using mass loss method. The IE_{ML}% decreases from 95.8% to 80.6% as the temperature increases.

Table 4. Effect of temperature on the inhibition efficiency of OESL using 2.5 g/L

Inhibitor	Temperature	Mass loss (mg)	IE_{ML}%
Blank	293	72.9	-
	303	87.4	-
	313	97.8	-
	323	116.7	-
OESL	293	3.5	95.2
	303	8.5	90.3
	313	15.1	84.5
	323	26.6	77.2

These results exhibited that OESL can be used effectively to minimize the corrosion reactions at normal and moderate temperatures. Results presented in Table 4 prove that the values of mass loss increase as the temperature increases in both the blank and inhibited solutions.

The mass loss values were exploited to calculate the activation energy (E_a) using Equation 7 and Figure 6(a). The entropy (ΔS) and enthalpy (ΔH) changes are usually determined using Equation 8.

$$\ln \mathrm{ML} = \ln \mathrm{A} - \frac{\mathrm{E_a}}{\mathrm{RT}} \quad (7)$$

$$\ln\left(\frac{ML}{T}\right) = \frac{-\Delta \mathrm{H}}{\mathrm{RT}} + \ln\frac{\mathrm{k_B}}{\mathrm{h}} + \frac{\Delta \mathrm{S}}{\mathrm{R}} \quad (8)$$

E_a stands for activation energy of the corrosion process, k_B is the Boltzmann constant, T is the absolute temperature, A is the frequency factor, and h is Planck's constant.

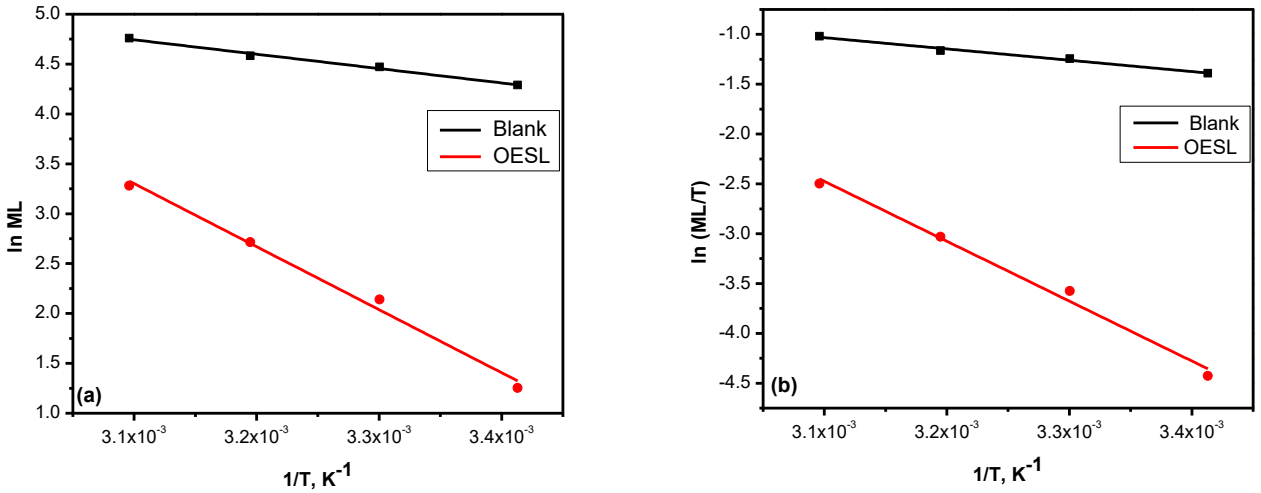

Figure 6. Plot of (a) Arrhenius and (b) Erying models for blank and OESL (2.5 g/L)

Values of ΔS and ΔH in the inhibited and blank solutions were calculated from the intercept and slope of Figure 6(b) and presented in Table 5.

Table 5. The values of activation parameters for CS in HCl (1.0 M) in the absence and presence of 2.5 g/L of OESL

	E_a, kJ/mol	ΔS, J/mol	ΔH, kJ/mol
Blank	37.8	452.2	-17.7
2.50 g/L of OESL	53.2	517.6	-23.1

Results reveal that E_a value in the inhibited solutions is greater than that in the blank solution indicating that the corrosion process became harder after in the presence of OESL. Table 5 also shows that The large and negative value of ΔH in the presence of the OESL designates that the corrosion is an exothermic process, suggesting that the ionization of steel surface is slow [11] in the presence of OESL and this is good agreement with results displayed in Table 4. The entropy change (ΔS) has large and positive value indicating that during the rate-determining step, the activated complex is formed by

an association rather than a dissociation step [27], proving that an increase in the disorder takes place on going from reactants to the activated complex.

3.5. SEM study

The morphology of the surface of the CS sample was examined using Scanning Electron Microscopy (SEM) technique. The CS surface before and after immersion in 1.0 M HCl are displayed in Figure 7. Figure 7a displays an extremely scratched and surface mostly due to the presence of aggressive corrosion medium. However, a smooth surface was observed as shown in Figure 7b in the presence of the OESL. This observation is due to adsorption of protective film layer on the CS surface, hence decreasing the rigorousness of corrosion. However, few slight scratches are still observed after adding OESL.

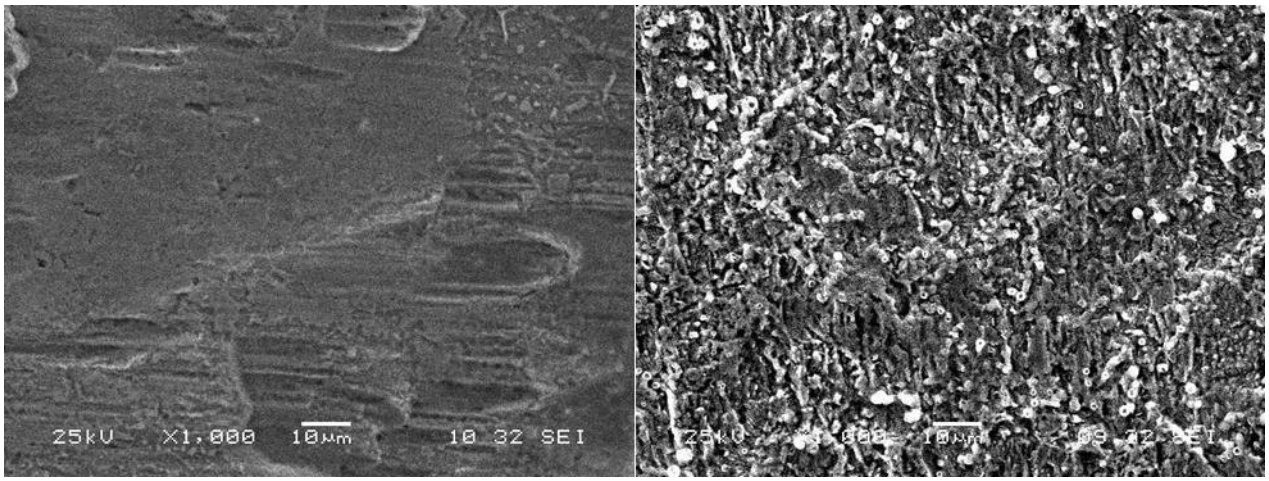

(a) (b)

Figure 7. SEM image for (a) CS surface after addition of 2.5 g/L of OESL (b) CS surface without OESL and the immersion time was 6 hrs at 298K

3.6 Comparison with other natural products

Table 4 displays the inhibition efficiencies, isotherm model and activation energies of several natural extracts that used as corrosion inhibitors. It clear that OESL has the highest inhibition efficiency among all these extracts (95.8%). It is also observed that all materials obey the Langmuir isotherm model. Furthermore, the corrosion process in the presence of OESL has the greatest value of activation energy. This indicates that the corrosion process in the presence of OESL became more difficult than that in the presence of all other extracts.

Table 4. Comparison between various natural products as corrosion inhibitors

Inhibitor	IE%	Isotherm model	E_a, kJ/mol	Ref.
Acacia tortilis leaves	88.7	Langmuir	47.2	[4]
Acacia tortilis barks	70.2	Langmuir	42.6	[4]
Juniperus procera leaves	85.7	Langmuir	25.7	[5]
Coleus forskohlii leaves	87.8	Langmuir	42.0	[10]
Oil from *Moringa peregrina* leaves	68.0	Langmuir	**	[11]
Carob seed oil	81.7	Langmuir	38.6	[28]
ginkgo biloba leaves	80.7	**	**	[29]
Chenopodium Ambrosioides	94.0	Langmuir	33.7	[30]
OESL	95.8	Langmuir	53.2	This study

** Not reported

4. CONCLUSION

This work presents inhibition properties of the oil extracted from the leaves of *Eruca sativa* in 1.0 M HCl solutions. The inhibition mechanisms were explored to reveal the effectiveness of OESL via several conventional and electrochemical experiments. The examined oil displayed good inhibitive potential when compared with other natural inhibitors. PDP results revealed that OESL acts as mixed type corrosion inhibitor. The polarization resistance increased when OESL is added to the corrosive solution and this consequently reduced the values of double-layer capacitance. The adsorption of OESL on the CS surface was found to follow Langmuir model.

CONFLICT OF INTEREST
The author declares that he has no conflict of interest.

ACKNOWLEDGEMENTS
The author extend his appreciation to the Deanship of Scientific Research at King Khalid University for funding this work through research groups program under grant number R.G.P.2/56/42.

References

1. M. Benahmed, I. Selatnia, N. Djeddi, S. Akkal, H. Laouer, *Chem. Afr*. 3 (2020) 251.
2. M.A. Quraishi, R. Sardar, *Corrosion,* 58 (2002) 748.
3. I. Ali, J. Yisa, J. O. Jacob, *Trends in Science and Technology Journal*, 4 (2019) 284.
4. I. H. Ali, A. M. Idris, M. H. A. Suliman, *Int. J. Electrochem. Sci*., 14 (2019) 6406.
5. M. H.A. Suleiman, I. H. Ali, *Int. J. Electrochem. Sci.,* 13 (2018) 3910.
6. N. S Patel, J. Hadlicka, P. Beranek, R. Salghi, H. Bouya, H. A. Ismat, B. Hammouti, *Port. Electrochim. Acta*, 32 (2014) 395.
7. I.H. Ali, *Int. J. Electrochem. Sci*., 11(2016) 2130.

8. P. Parthipan, P. Elumalai, J. Narenkumar, L. L. Machuca, K. Murugan, O. P. Karthikeyan, A. Rajasekar, A. sativum, *International Biodeterioration & Biodegradation*, 132 (2018) 66.
9. P. C. Okafor, E. E. Ebenso, U. J. Ekpe, *Int. J. Electrochem. Sci.,* 5 (2010) 978.
10. I. H. Ali, R. Marzouki, Y. B. Smida, A. Brahmia, M. F. Zid, *Int. J. Electrochem. Sci*., 13 (2018) 11580.
11. I. H. Ali, M. I. Khan, A. M. Alraih, M. K. Almesfer, A. Elkhaleefa, S. M. Dmour, M. Rehan, *Int. J. Electrochem. Sci.,* 16 (2021) 210842.
12. R. T. Loto, E. H. Mbah, J. I. Ugada, *South African Journal of Chemical Engineering*, 35 (2021) 159.
13. P. B. Raja, M. G. Sethuraman, *Materials Letters*, 62 (2008) 2977.
14. O. Sanni, A. Popoola, *J. Fail. Anal. and Preven.*, 18 (2018) 1191.
15. M. Omotioma, O. D. Onukwuli, *Int. J. Electrochem. Sci*., 14 (2016) 103.
16. G. ASTM, G 31-72, Standard practice for laboratory immersion corrosion testing of metals, 1990.
17. M. Damej, S. Kaya, B. El-Ibrahimi, H-S. Lee, A. Molhi, G. Serdaroğlu, M. Benmessaoud, I. H. Ali, S. EL Hajjaji, H. Lgaz, *Surfaces and Interfaces*, 24 (2021) 101095.
18. H. Li, S. Zhang, Y. Qiang, *J. Mol. Liq*., 321 (2021) 114450.
19. T. Z. Abdul-Jalil, *International Journal of Pharmacognosy and Phytochemical Research*, 8 (2016) 1722.
20. A. Singh, K. Ansari, D.S. Chauhan, M. Quraishi, S. Kaya, *Sustain. Chem. Pharm.*, 16 (2020), 100257.
21. A. A. Abdulridha, M. A. A. Hay Allah, S. Q. Makki, Y. Sert, H. E. Salman, A. A. Balakit, *J. Mol. Liq.*, 315 (2020), 113690.
22. M. Chafiq, A. Chaouiki, M. R. Albayati, H. Lgaz, R. Salghi, S.K. AbdelRaheem, I. H. Ali, S. K. Mohamed, I.-M. Chung, *J. Mol. Liq.*, 320 (2020) 114442.
23. K. Ansari, D.S. Chauhan, M. Quraishi, M.A. Mazumder, A. Singh, *Int. J. Biol. Macromol.*, 144 (2020) 305.
24. M. Abdallah, K. A. Soliman, Arej S. Al-Gorair, A. Al Bahir, J. H. Al-Fahemi, M. S. Motaweab, S. S. Al-Juaid, *RSC Adv*., 11 (2021) 17092.
25. A. S. Fouda, S. A. Abd El-Maksoud, E. H. El-Sayed, H. A. Elbaz, A. S. Abousalem, *RSC Adv*., 11 (2021) 13497.
26. P. Singh, M. Makowska-Janusik, P. Slovensky and M. A. Quraishi, *J. Mol. Liq.,* 71 (2016) 220.
27. R. Salghi, S. Jodeh, E. E. Ebenso, H. Lgaz, D. Ben Hmamou, I. H. Ali, M. Messali, B. Hammouti, N. Benchat, *Int. J. Electrochem. Sci.,* 12 (2017) 3309.
28. D. B. Hmamou, R. Salghi, A. Zarrouk, O. Benali, F. Fadel, H. Zarrok, B. Hammouti, *International Journal of Industrial Chemistry*, 3 (2012) 25.
29. G. Chen, M. Zhang, J. Zhao, R. Zhou, Z. Meng, J. Zhang, *Chemistry Central Journal*, 7 (2013) 83.
30. L. Bammou, M. Belkhaouda, R. Salghi, O. Benali, A. Zarrouk, H. Zarrok, B. Hammouti, *Journal of the Association of Arab Universities for Basic and Applied Sciences*, 16 (2014) 83.